Radiotherapy and Oncology 211 (2025) 111097

Contents lists available at ScienceDirect

Radiotherapy and Oncology

journal homepage: www.thegreenjournal.com

Original Article

Prospective clinical trial of upright image-guided proton therapy for locally recurrent head and neck and brain malignancies☆

Philip Blumenfeld [a,1], Alexander Pryanichnikov [b,c,*,1], Yair Hillman [a], Ella Wajnryt [a], Aviad Berger [a], Shimshon Winograd [d], Marc Wygoda [a], Ayman Salhab [a], Marcel Fang [a], Jon Feldman [a], Aron Popovtzer [a]

[a] Sharett Institute of Oncology, Hadassah Medical Center, Hebrew University of Jerusalem, Jerusalem, Israel
[b] Institute of Biomedical Engineering, Karlsruhe Institute of Technology (KIT), Karlsruhe, Germany
[c] Division of Biomedical Physics in Radiation Oncology, German Cancer Research Center (DKFZ), Heidelberg, Germany
[d] P-Cure Ltd./Inc, Shilat, Israel

ARTICLE INFO

Keywords:
Radiotherapy
Adaptive radiotherapy
Proton therapy
Image guidance
Upright CT
Upright treatments

ABSTRACT

Purpose: The advent of commercially available vertical CT systems has renewed interest in gantry-less proton therapy (PT), in which patients are treated in an upright position using a fixed beamline and robotic positioning. This study evaluates the feasibility, safety, and preliminary efficacy of novel gantry-less image-guided adaptive PT (IGAPT) for recurrent head and neck (HN) and brain malignancies.

Materials and methods: A planned interim analysis was performed on 20 adult patients with recurrent HN (80 %) and brain (20 %) cancers, median age 62 years, with Eastern Cooperative Oncology Group (ECOG) performance status $\leq$2. Patients underwent upright and supine imaging and simulation, followed by treatment planning comparing upright PT to conventional supine intensity-modulated radiotherapy (IMRT). Dosimetric analyses focused on organ-at-risk (OAR) sparing and target coverage. Toxicities were assessed prospectively every three months using the Common Terminology Criteria for Adverse Events (CTCAE).

Results: Gantry-less PT demonstrated significant dosimetric advantages over photon IMRT, including reduced doses to critical OARs including brainstem (6 Gy(RBE) vs. 19.1 Gy; $p < 0.001$) and spinal cord (12.5 Gy(RBE) vs. 18.3 Gy; $p < 0.006$). At 3-month follow-up ($n = 14$), a complete response was observed in 64.3 % of evaluable patients and a partial response in 21.4 %. Most toxicities were mild-to-moderate (grades 1–2), primarily dermatitis (55 %), fatigue (45 %), and mucositis (31.3 %). Grade 3 toxicities occurred in four patients (20 %). There were no device-related deaths.

Conclusions: This first clinical evaluation of a novel gantry-less IGAPT system confirms its feasibility, safety, and promising efficacy for recurrent HN and brain cancer, with superior dosimetry and high local control rates. Its cost-effective design may improve global access to the IGAPT.

Introduction

Recurrent head and neck (HN) and brain malignancies present significant clinical challenges, particularly when they occur within previously irradiated fields. Re-irradiation remains essential for effective local disease control and prolonged survival despite the increased risk of severe toxicity, necessitating careful balance between therapeutic gain and radiation-induced damage to critical structures, including the brainstem, spinal cord, optic pathways, and other adjacent sensitive tissues [1,2,3].

Proton therapy (PT) offers distinct advantages in treating recurrent HN and brain malignancies due to its favorable dosimetric properties characterized by the Bragg peak [4,5]. This physical characteristic allows maximum radiation dose delivery precisely to the tumor while minimizing exposure to healthy tissues, thereby reducing toxicity compared to photon therapy, especially in re-irradiation settings

☆ This article is part of a special issue entitled: 'Reirradiation' published in Radiotherapy and Oncology.

* Corresponding author.
E-mail address: alexander.pryanichnikov@kit.edu (A. Pryanichnikov).

[1] These authors contributed equally to this work and share first authorship.

https://doi.org/10.1016/j.radonc.2025.111097
Received 17 March 2025; Received in revised form 22 July 2025; Accepted 24 July 2025
Available online 11 August 2025

Table 1
Patient data: disease and treatment characteristics.

Patient #	Age	Gender	Primary Tumor Location	Histology	Irradiated Area	Dose Fractionation
1	85	F	H/N	Buccal Mucosa cancer	Neck, tongue	70 Gy in 35 fractions
2	79	F	H/N	Buccal Mucosa cancer	Neck	70 Gy in 35 fractions
3	59	M	H/N	Recurrent sinus malignant transformation of inverted papilloma	Rt eye, Rt neck	62.5 Gy in 25 fractions to the neck 57.5 Gy in 23 fractions to the eye
4	47	M	Brain	Glioblastoma	Brain	35 Gy in 10 fractions
5	61	M	H/N	sinus mauxiliary carcinoma	Right maxillary sinus	66 Gy in 33 fractions
6	62	F	H/N	Laryngeal SCC	Rt neck	68 Gy in 36 fractions
7	67	F	H/N	Tongue Cancer	Base of tongue/ tongue	70 Gy in 35 fractions
8	78	F	H/N	Salivary gland carcinoma	Neck	70 Gy in 35 fractions
9	68	M	H/N	Tonsil cancer	Base of tongue/ tonsil	46.25 Gy in 18.5 fractions
10	46	F	H/N	Nasopharynx cancer	Nasopharynx/neck	54 Gy in 18 fractions
11	88	F	H/N	Tongue Cancer-lip and oral cavity SCC	Oral cavity, cheek	60 Gy in 30 fractions to the oral cavity48Gy in 16 fractions to the cheek
12	77	M	H/N	Tonsil/tongue base SCC with bilateral adenopathy	Left parotid/neck	70 Gy in 35 fractions
13	62	F	H/N	Hypopharynx cancer	Oropharynx	70 Gy in 36 fractions
14	62	F	Brain	Oligodendroglioma	Brain	54 Gy in 27 fractions
15	43	F	Brain	Glioblastoma	Brain	35 Gy in 10 fractions
16	57	F	H/N	Malignant neoplasm of oropharynx	Oropharynx	70 Gy in 35 fractions
17	41	M	Brain	Glioblastoma	Brain	36 Gy in 10 fractions
18	79	F	H/N	larynx malignancy	Larynx	70 Gy in 35 fractions
19	39	F	H/N	lateral wall of Oropharynx	Oropharynx	18 Gy in 9 fractions
20	85	M	H/N	Malignant neoplasm of skin involved parotid	Ear canal and parotid	70 Gy in 35 fractions

[6,7,8]. Despite clear dosimetric advantages and growing clinical adoption, the high capital cost of conventional PT facilities—dominated by large, expensive rotating gantry systems—has limited global accessibility [9,10,11,12,13].

Recent technological advances have enabled the application of image-guided adaptive (IGA) workflow, previously established only for supine positioning [14,15], to upright gantry-less PT systems. These systems consist of a fixed horizontal beamline, patient rotation via robotic chair-based positioning, and integrated vertical computed tomography (CT). Such configurations dramatically reduce both cost and space requirements compared to conventional gantry-based systems, potentially increasing the feasibility of widespread implementation of IGAPT [16,17,18]. Previous work has reported the commissioning of the first such system [12]. It has also been demonstrated the level of accuracy and reproducibility of upright patient positioning for head and neck cancer compared to the supine facilities [13]. Other studies have also established the clinical viability of upright proton treatment positions for complex anatomical sites, with promising efficacy and manageable toxicity profiles [6,16,19,20].

Building on this foundation, we initiated a prospective clinical trial to evaluate gantry-less IGAPT for locally recurrent HN and brain malignancies. This study evaluates the feasibility, safety, early clinical outcomes, and dosimetric advantages of upright fixed-beamline IGAPT compared to standard supine, photon-based intensity-modulated radiation therapy (IMRT). This interim analysis aims to demonstrate the potential of gantry-less PT to achieve superior dosimetry and favorable clinical outcomes in complex re-irradiation scenarios.

Materials and methods

This prospective trial evaluated the efficacy, toxicity, quality of life (QOL), and treatment planning parity in adult patients with recurrent HN and brain cancers receiving upright gantry-less IGAPT.

Study Objectives

The primary objectives were to assess local control at 3 months post-treatment, physician-reported acute toxicity, and to compare upright IGAPT with supine photon-based IMRT for OAR sparing. Secondary objectives focused on long-term toxicity (3 months post-treatment), and quality of life. QOL was assessed using validated patient-reported questionnaires such as the EORTC QLQ-C30 and site-specific tools such as the QLQ-H&N35 for head and neck tumors and the QLQ-BN20 for brain tumors. Acute toxicities were graded according to CTCAE v5.0 criteria.

Patient Selection

Patients were eligible if they were $\geq$ 18 years of age, had histologically or radiologically confirmed recurrent HN or brain malignancies, and had previously received radiotherapy. Inclusion required an ECOG performance status $\leq$ 2 and life expectancy $\geq$ 6 months. PT treatment plans had to show superior dosimetric results compared to IMRT to qualify patients for inclusion. Patients were excluded if they had untreated primary tumors, photon-based plans with superior dosimetry, or a history of other malignancies within three years. All participants provided informed consent, and female patients underwent pregnancy testing prior to treatment initiation.

Twenty adult patients with recurrent HN and brain malignancies were included in this interim analysis. The median age was 62 years (range, 39–88) and most participants were female (65 %). The majority (95 %) had an ECOG performance status of 0–1, while one patient (5 %) had an ECOG status of 2. Recurrent tumors were primarily head and neck malignancies (80 %) involving the oral cavity (n = 4), oropharynx (n = 3), larynx/hypopharynx (n = 3), nasopharynx (n = 1), sinonasal regions (n = 2), and salivary glands (n = 1). Brain malignancies (20 %) included oligodendroglioma (n = 1) and glioblastoma (n = 3). The median interval from initial radiotherapy to re-irradiation was 1.67 years (range, 0.44–25.4 years), with median prior RT doses of 70 Gy for HN cancers and 60 Gy for brain tumors. Detailed data presented in Table 1.

This study was conducted following the guidelines of the Declaration of Helsinki and was approved by the Institutional Review Board of Hadassah Medical Center.

Proton Therapy System

Patients were treated at the Sharett Institute of Oncology, Hadassah Medical Center, using the P-Cure Proton Therapy System (P-Cure Ltd., Shilat, Israel) as previously described [12,13]. The system integrates a compact proton synchrotron that delivers pencil beam scanning proton therapy with energies ranging from 50 to 250 MeV The system has been commissioned for an energy range of 50 to 70 MeV, which is different from what was previously published [12]. The proton beam spot sizes varied from 2.8 mm (for the highest energy) to 7.7 mm (for the lowest energy). The treatment room houses a fixed horizontal beamline and robotic patient positioning with a six-degrees-of-freedom (6-DoF) robotic chair (Leoni Orion, Montigny-le-Bretonneux, France). The imaging system includes a vertical CT scanner (Philips Brilliance Big Bore) angled 20° with respect to the vertical axis and an orthogonal kV X-ray system for accurate verification of patient positioning [12,13].

Pretreatment Evaluation and Simulation

Comprehensive pretreatment imaging, including PET-CT for HN malignancies and MRI for brain malignancies, was performed within one month prior to treatment. The pretreatment evaluation included detailed medical history, physical examination, and laboratory tests (CBC, chemistry panel). Baseline quality of life questionnaires (EORTC QLQ-C30, site-specific QLQ-H& N35, and QLQ-BN20) were completed. All patients underwent two separate simulation sessions: conventional supine CT for IMRT planning and vertical CT using the robotic chair system for PT planning. Five-point thermoplastic masks were used for immobilization in both positions. Patients completed visual analog scale questionnaires to report comfort levels as previously published [13].

Daily Positioning Verification

Daily positioning verification was integrated into the treatment workflow by acquiring a low–dose upright CT immediately after immobilisation on the robotic chair. Automatic registration yielded six–degree–of–freedom offsets that were applied to the chair before irradiation. The translational motion is determined by three axes: two orthogonal axes (X, Y) parallel to the floor of the room and a Z-axis orthogonal to them. All registration results and correction vectors were archived, allowing retrospective analysis of 548 fractions in the current cohort; the methodology is identical to that described in the initial ten–patient validation study [13] and therefore permits a direct comparison.

Treatment Planning and Delivery

Target volumes and OARs were delineated according to Radiation Therapy Oncology Group (RTOG) guidelines. Dosimetric analyses compared upright proton plans with standard photon IMRT, emphasizing critical structure sparing while ensuring adequate target coverage.

Treatment plans followed ICRU Reports #50 and #62 recommendations. Doses for recurrent HN malignancies were predominantly 60–70 Gy(RBE) delivered in 30–35 fractions, with some cases using hypofractionated schedules of 45–50 Gy(RBE) in 15–20 fractions. Recurrent brain tumors were treated with either conventional (54 Gy (RBE) in 30 fractions) or hypofractionated schedules (35 Gy(RBE) in 10 fractions). All treatment plans were independently reviewed. The treatment planning system used in this study was the RayStation 2023B (RaySearch Laboratories, Stockholm, Sweden).

In the study cohort, 70 % required at least one offline adaptive replanning session (ranging from one to three). Triggers for replanning included tumor progression, significant anatomic changes, and treatment complications. Replanning was performed between fractions 5 and 30, with dose escalation proving particularly beneficial in sino-nasal cases to mitigate toxicity while maintaining tight margins.

Table 2
Registered mean ± SD shifts of patient positioning verification for full cohort (20 patients).

Patient #	⟨Δχ⟩, mm	⟨Δy⟩, mm	⟨Δz⟩, mm	⟨Δφχ⟩, deg	⟨Δ φy⟩, deg	⟨Δ φz⟩, deg
1	1.53 ± 3.43	−1.63 ± 0.93	−8.51 ± 3.78	−1.47 ± 0.87	0.61 ± 0.89	1.64 ± 1.00
2	0.94 ± 1.06	−2.64 ± 0.98	−1.48 ± 1.27	−0.82 ± 0.49	0.44 ± 0.49	0.30 ± 0.38
3	0.21 ± 4.06	−5.37 ± 2.46	3.19 ± 5.92	−0.03 ± 1.04	1.17 ± 1.44	0.85 ± 1.44
4	−1.45 ± 1.79	−2.88 ± 2.47	−2.74 ± 2.30	−0.16 ± 1.15	0.03 ± 0.44	−0.40 ± 1.15
5	−4.92 ± 9.67	−1.58 ± 3.05	−2.83 ± 2.25	1.06 ± 1.08	0.38 ± 0.99	0.77 ± 0.98
6	−3.47 ± 2.72	−0.27 ± 1.86	1.81 ± 5.38	0.19 ± 0.70	0.13 ± 0.86	0.74 ± 1.04
7	−4.29 ± 4.98	−2.20 ± 2.36	2.09 ± 5.60	−1.09 ± 1.07	1.35 ± 2.13	0.41 ± 1.24
8	0.39 ± 1.57	−6.97 ± 3.05	9.55 ± 8.11	1.32 ± 0.70	−0.16 ± 0.75	−1.18 ± 0.37
9	2.09 ± 3.83	0.10 ± 2.80	0.24 ± 3.47	0.85 ± 1.38	−0.23 ± 1.56	−0.40 ± 1.67
10	−1.96 ± 2.13	−3.77 ± 1.45	−1.74 ± 1.80	−0.20 ± 0.60	−1.69 ± 0.56	0.13 ± 0.53
11	−9.55 ± 2.75	−0.78 ± 1.15	−1.22 ± 4.26	0.45 ± 0.85	−0.96 ± 1.01	1.74 ± 1.16
12	−0.34 ± 3.93	−2.18 ± 1.39	4.21 ± 4.08	−0.19 ± 0.64	−0.76 ± 0.52	−0.12 ± 0.87
13	−0.99 ± 2.38	−5.05 ± 4.66	2.80 ± 3.97	−2.34 ± 2.31	−0.00 ± 0.85	−0.61 ± 1.11
14	0.06 ± 4.74	−3.73 ± 2.16	−2.66 ± 2.99	−1.60 ± 1.06	−0.62 ± 1.17	0.05 ± 1.08
15	1.85 ± 1.81	−2.52 ± 1.85	10.48 ± 3.45	−2.38 ± 2.05	−0.79 ± 0.51	0.64 ± 0.86
16	−4.98 ± 4.49	−4.07 ± 1.71	−2.55 ± 2.24	−0.62 ± 0.60	0.02 ± 0.59	0.19 ± 0.75
17	−7.94 ± 3.97	−1.57 ± 0.40	−1.89 ± 3.53	1.23 ± 0.53	0.40 ± 0.70	−1.21 ± 0.58
18	3.57 ± 4.25	−2.59 ± 1.05	−6.15 ± 3.74	−0.69 ± 0.89	−2.50 ± 1.17	0.16 ± 0.79
19	3.57 ± 2.63	−0.34 ± 1.27	−4.40 ± 3.24	−0.98 ± 0.57	−0.32 ± 0.71	−1.87 ± 0.91
20	−1.87 ± 4.87	−2.68 ± 2.29	−0.59 ± 4.28	−2.14 ± 1.52	−0.94 ± 1.42	−2.06 ± 2.01

Comparative Dosimetric Substudy

In addition to the dosimetric comparison between supine IMRT and upright PT, an embedded planning substudy was performed on four representative patients (25 % of the current cohort), who were selected to span diverse primary sites and target geometries. Four additional treatment plans were created: supine photon IMRT (S–Ph), upright photon IMRT (Up–Ph), supine PT (S–P) using the gantry–based beamline model, and upright PT (Up–P) using a fixed horizontal beamline. All plans were generated in RayStation 2023B using identical contour sets and robust optimisation parameters (±3 mm setup, ±3 % range for protons). Dose–volume metrics followed ICRU #50/#62 recommendations: $D_{95\ \%}$, $D_{2\%}$, $V_{95\ \%}$, the ICRU 83 homogeneity index (HI), and the RTOG conformity index (CI). OARs were evaluated using structure-specific endpoints (e.g., brain–stem and spinal–cord D_{5cc}, parotid D_{mean}, etc.). The dose prescriptions reflected the clinical Rx for each patient (56–70 Gy for photons or Gy(RBE) for protons).

Treatment Verification and Follow-up

Patients were evaluated weekly during treatment. To verify positional accuracy, daily interfractional positioning was assessed using 3D/3D CT registration, with subsequent treatment plan adaptation if needed. Intrafractional accuracy at the treatment isocenter was

Table 3
Dosimetric comparison: upright PT vs. supine IMRT full cohort (20 patients).

Organ at Risk Constraint	Protons	Photons	P-Value
Oral Cavity (Mean, 15pts)	5.6 Gy(RBE)	18.5 Gy	$p < 0.001$
C/l Parotid (Mean, 12pts)	0.2 Gy(RBE)	6.95 Gy	$p < 0.001$
C/l Submandibular Gland (Mean, 11pts)	0.3 Gy(RBE)	7.3 Gy	$p < 0.001$
Constrictor Muscles (Mean, 4 pts)	11.4 Gy(RBE)	21.1 Gy	$p < 0.01$
C/l cochlea (Mean, 3pts)	0 Gy(RBE)	7 Gy	$p < 0.01$
Brainstem (Maximum, 10 pts)	6 Gy(RBE)	19.1 Gy	$p < 0.001$
Brain (V5Gy, 4 pts)	264.5 cc	618 cc	$p < 0.001$
Brainstem D_{2cc}	5.8 Gy(RBE)	14.5 Gy	$p < 0.004$
Spinal Cord D_{max} (14 pts)	12.5 Gy(RBE)	18.3 Gy	$p < 0.006$
Spinal Cord D_{5cc} (14pts)	0.8 Gy(RBE)	12.6 Gy	$p < 0.001$

confirmed using orthogonal 2D/3D radiographic registrations [13]. Post-treatment evaluations occurred at one week, one month, and three months, including clinical assessments, imaging studies (PET-CT for HN cancers, MRI for brain tumors), laboratory tests (CBC, chemistry panels) and QOL assessments. All deaths were reviewed by the Data Safety Monitoring Board (DSMB) to evaluate their association with the treatment, the device, or other causes.

Statistical Methods

Local control and survival outcomes were analyzed using the Kaplan-Meier method. Dosimetric comparisons between proton and photon plans were performed using paired t-tests. Acute toxicities and quality of life data were summarized descriptively. Statistical significance was set at $p < 0.05$.

Results

The clinical intent of the twenty patients was curative in 85 % of cases and palliative in 15 % of cases. Concurrent chemotherapy was administered to 60 % of the patients, while 40 % received radiation alone.

Inter-fraction patient position was verified before every fraction by 3D/3D registration between the daily upright CT and the reference planning CT. Across 20 patients we acquired and analyzed 548 verification scans (Table 2). The mean corrective shifts for the full cohort were $\langle\Delta\chi\rangle = -1.38 \pm 3.58$ mm, $\langle\Delta y\rangle = -2.64 \pm 1.81$ mm, $\langle\Delta z\rangle = -0.12 \pm 4.67$ mm, $\langle\Delta\varphi_\chi\rangle = -0.48 \pm 1.15$ deg, $\langle\Delta\varphi_y\rangle = -0.22 \pm 0.91$ deg, $\langle\Delta\varphi_z\rangle = -0.01 \pm 1.02$ deg The full distributions are shown in Supplementary Figure S1. Compared with the previously published ten-patient series, in which the dominant displacement was -3.7 ± 3.5 mm along the Y axis, the present data demonstrate both a larger sample and a narrower variability band, reflecting gained experience in chair alignment since the earlier report.

PT delivered with the upright, chair-based system demonstrated significant dosimetric advantages over standard photon-based IMRT. As

Table 4
Target–volume coverage and organ–at–risk dose metrics for four representative patients planned with supine photon IMRT (S–Ph), upright photon IMRT (Up–Ph), supine proton therapy (S–P) and upright proton therapy (Up–P).

Target-volume Coverage																
Dose Index	Patient A				Patient B				Patient C				Patient D			
	S-Ph	Up-Ph	S-P	Up-P	S-Ph	Up-Ph	S-P	Up-P	S-Ph	Up-Ph	S-P	Up-P	S-Ph	Up-Ph	S-P	Up-P
$D_{95\%}$	56.47 Gy	56.14 Gy	55.63 Gy (RBE)	55.49 Gy (RBE)	60.45 Gy	60.93 Gy	57.38 Gy (RBE)	60.56 Gy (RBE)	52.34 Gy	52.47 Gy	52.65 Gy (RBE)	52.37 Gy (RBE)	54.24 Gy	49.64 Gy	51.68 Gy (RBE)	51.86 Gy (RBE)
$D_{2\%}$	59.18 Gy	58.44 Gy	58.24 Gy (RBE)	58.05 Gy (RBE)	72.39 Gy	73.39 Gy	73.11 Gy (RBE)	73.45 Gy (RBE)	54.08 Gy	54.12 Gy	54.08 Gy (RBE)	53.92 Gy (RBE)	57.05 Gy	57.94 Gy	56.51 Gy (RBE)	56.51 Gy (RBE)
$V_{95\%}$	99.99	100.00	99.99	99.92	23.91	32.34	35.69	38.85	100.00	100.00	100.00	100.00	99.98	94.01	95.40	95.28
HI	0.05	0.04	0.05	0.05	0.22	0.21	0.34	0.22	0.04	0.03	0.03	0.03	0.06	0.30	0.23	0.26
CI	0.99	0.97	0.88	0.86	0.15	0.22	0.21	0.22	0.99	1.00	1.00	0.99	0.98	0.86	0.76	0.87

Dose to OARs					
Dose Index	**OAR**	**S-Ph**	**Up-Ph**	**S-P**	**Up-P**
Patient A					
D_{5cc}	Brain Stem	4.14 Gy	20.11 Gy	5.52 Gy(RBE)	5.83 Gy(RBE)
	Spinal Canal	22.40 Gy	19.28 Gy	9.58 Gy(RBE)	7.57 Gy(RBE)
Mean dose	Larynx	4.26 Gy	5.87 Gy	4.87 Gy(RBE)	4.96 Gy(RBE)
	Mandible Bone	12.51 Gy	20.03 Gy	10.87 Gy(RBE)	11.75 Gy(RBE)
	Oral Cavity	16.74 Gy	26.29 Gy	9.07 Gy(RBE)	9.11 Gy(RBE)
	Parotid L	23.35 Gy	24.99 Gy	16.76 Gy(RBE)	16.65 Gy(RBE)
	Parotid R	9.21 Gy	13.65 Gy	2.02 Gy(RBE)	2.04 Gy(RBE)
Patient B					
Mean dose	Constrictor Muscles	32.90 Gy	38.64 Gy	23.21 Gy(RBE)	33.21 Gy(RBE)
	Larynx	46.93 Gy	51.17 Gy	40.95 Gy(RBE)	45.10 Gy(RBE)
	Oral Cavity	17.84 Gy	18.50 Gy	8.21 Gy(RBE)	5.31 Gy(RBE)
	Parotid L	18.29 Gy	23.79 Gy	21.94 Gy(RBE)	22.13 Gy(RBE)
	Parotid R	7.37 Gy	6.93 Gy	1.89 Gy(RBE)	2.33 Gy(RBE)
Patient C					
Mean dose	Constrictor Muscles	15.32 Gy	17.55 Gy	9.09 Gy(RBE)	9.52 Gy(RBE)
	Larynx	10.24 Gy	12.57 Gy	6.59 Gy(RBE)	6.58 Gy(RBE)
	Mandible	11.13 Gy	8.45 Gy	7.71 Gy(RBE)	5.89 Gy(RBE)
	Oral Cavity	7.31 Gy	5.95 Gy	0.72 Gy(RBE)	0.73 Gy(RBE)
Patient D					
Mean dose	Mandible	26.47 Gy	27.15 Gy	17.43 Gy(RBE)	18.16 Gy(RBE)
	Oral Cavity	33.14 Gy	30.59 Gy	17.21 Gy(RBE)	17.53 Gy(RBE)
	Parotid L	15.99 Gy	13.47 Gy	12.85 Gy(RBE)	12.98 Gy(RBE)
	Parotid R	41.46 Gy	40.25 Gy	45.12 Gy(RBE)	45.83 Gy(RBE)
	Spinal Cord	21.12 Gy	16.91 Gy	13.00 Gy(RBE)	11.04 Gy(RBE)

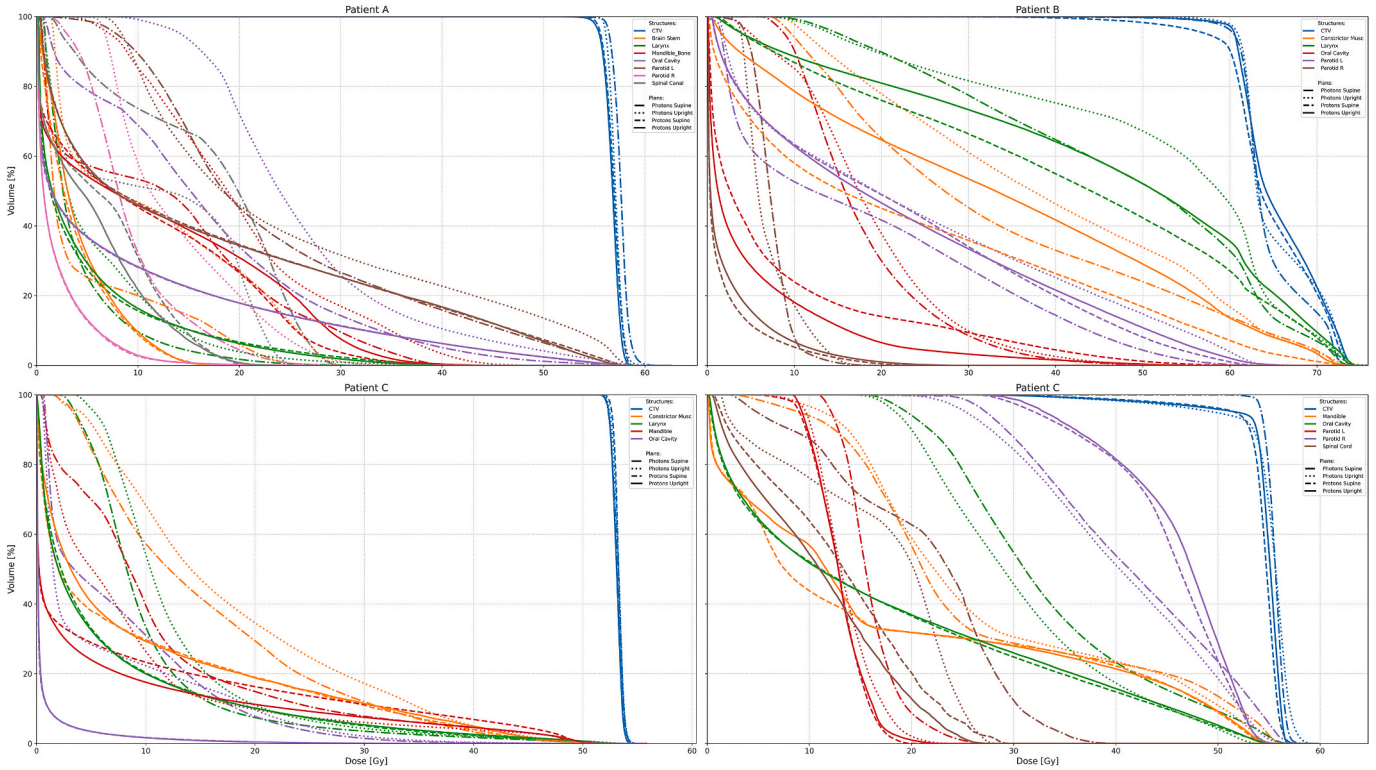

Fig. 1. Cumulative dose–volume histograms for the planning target volume and major organs at risk, comparing four delivery modalities: supine photon IMRT (S–Ph), upright photon IMRT (Up–Ph), supine proton therapy (S–P) and upright proton therapy (Up–P) in representative patients.

shown in Table 3, PT significantly reduced radiation exposure to OARs compared to IMRT, including maximum brainstem dose (6 Gy(RBE) vs. 19.1 Gy; $p < 0.001$) and maximum spinal cord dose (12.5 Gy(RBE) vs. 18.3 Gy; $p < 0.006$).

Data on the four selected patients are summarized in Table 4 and in composite DVHs (Fig. 1). Target coverage was comparable across modalities in patients A and C ($D_{95\ \%}$ within ± 1 % of Rx; $V_{95\ \%} \approx 100$ %). In patients with more complex geometries (patients B and D), supine and upright protons underperformed compared to supine photons in terms of conformity index (CI: 0.76–0.87 vs. 0.98) and heterogeneity index (HI: 0.22–0.34 vs. 0.06). Importantly, upright protons matched or exceeded supine protons in high-dose OAR sparing for three out of four cases. For patient A, the spinal cord D_{5cc} was 7.57 Gy(RBE) with upright protons versus 9.58 Gy(RBE) with supine protons. Patient C showed the largest incremental benefit; the mandible's mean dose decreased to 5.9 Gy (RBE) with upright protons versus 7.7 Gy(RBE) with supine protons (Table 4).

Pooled across the four patients, upright protons achieved median reductions relative to supine proton of 12 % for brain stem D_{max} and 18 % for oral cavity mean dose, while conformity decreased modestly by 0.08 absolute CI units (Table 4). This confirms that, for selected anatomies, upright delivery preserves the canonical proton sparing advantage and confers additional OAR benefit beyond supine gantry treatments.

Of the 14 patients who had imaging evaluations available at the 3-month follow-up, 64.3 % (n = 9) achieved a complete response (CR), demonstrating no evidence of disease on imaging. Partial responses (PR) were observed in 21.4 % of patients (n = 3), while 14.3 % (n = 2) had stable disease (SD). No patients experienced disease progression at the 3-month follow-up.

Six patients did not complete the three-month follow-up: one patient withdrew from the study and five patients died. One patient died during treatment after nine fractions due to underlying acute lymphoblastic leukemia, which was unrecognized at enrollment. Four additional deaths occurred during initial follow-up due to bleeding related to disease progression (n = 2), mental health issues (n = 1), and laryngeal edema related to initial radiation therapy (n = 1). After extensive review by the independent DSMB, none of these events were directly attributed to the proton therapy system.

Acute toxicities were graded according to the CTCAE version 5.0. Most acute toxicities were low grade (grade 1 or 2), with the most common fatigue (45 %), mucositis (31.3 %, and skin dermatitis (55 %). Notable grade 3 toxicities included one case of eye perforation, oral pain, dysphagia, and trismus. The detailed toxicity data is presented in Table 5.

Discussion

This interim analysis represents the first clinical evaluation of a novel gantry-less, chair-based proton IGAPT system for re-irradiation of head and neck and brain malignancies. The upright image-guided adaptive workflow demonstrated in this study addresses several critical challenges in contemporary proton therapy delivery while maintaining clinical efficacy and safety.

Three technical innovations distinguish this platform from conventional gantry-based proton therapy systems. First, the integrated vertical CT scanner enables on-site, real-time adaptive planning, a capability previously limited to supine configurations [14]. Second, a robotic six-degree-of-freedom chair provides submillimeter patient alignment without the spatial constraints and capital expense of a rotating gantry [12,13]. Third, embedding these elements in a fixed horizontal beamline significantly reduces the facility's footprint while preserving the well-established dosimetric advantages of proton therapy [6,12,17,18]. Since gantry construction and maintenance are major cost drivers, this architecture offers a more economical path to proton access [8,11].

The new positional data confirm and expand upon our previous findings. The current study of twenty patients demonstrates submillimeter average residuals in all directions except one, where the − 2.6 mm mean shift remains within the 3 mm clinical margin routinely applied in

Table 5
Acute toxic effects using CTCAE version 5.

Any grade toxicity (no. pts)	Any grade toxicity	Grade 1	Grade 2	Grade ≥ 3
Fatigue (20)	45 % (9)	35 % (7)	10 % (2)	**0**
Skin Dermatitis (20)	55 % (11)	20 % (4)	35 % (7)	**0**
Mucositis (16)	31.25 % (5)	6.25 % (1)	25 % (4)	**0**
Oral Pain (16)	31.25 % (5)	0	25 % (4)	**6.25 % (1)**
Dysphagia (16)	25 % (4)	6.25 % (1)	12.5 % (2)	**6.25 % (1)**
Edema (20)	25 % (5)	15 % (3)	5 % (1)	**5 % (1)**
Infection (20)	5 % (1)	0	0	**0**
Burn (20)	5 % (1)	5 % (1)	0	**0**
Oral thrush (16)	43.75 % (7)	25 % (4)	12.5 % (2)	**6.25 % (1)**
Trismus (16)	12.5 % (2)	0	6.25 % (1)	**6.25 % (1)**
Nausea (20)	10 % (2)	10 % (2)	0	**0**
Headaches (20)	10 % (2)	5 % (1)	5 % (1)	**0**
Alopecia (4)	50 % (2)	25 % (1)	25 % (1)	**0**
Local pain (20)	15 % (3)	0	15 % (3)	**0**
Dry skin (20)	5 % (1)	0	5 % (1)	**0**
Esophagitis (16)	6.25 % (1)	6.25 % (1)	0	**0**
Oral dysesthesia (16)	6.25 % (1)	0	6.25 % (1)	**0**
Oral bleeding (16)	6.25 % (1)	6.25 % (1)	0	**0**
Dry mouth (16)	12.5 % (2)	12.5 % (2)	0	**0**
Ear secretion (16)	6.25 % (1)	6.25 % (1)	0	**0**
Gait disbalance (4)	25 % (1)	25 % (1)	0	**0**
Hoarseness (16)	12.5 % (2)	6.25 % (1)	6.25 % (1)	**0**
Hearing impaired (20)	25 % (1)	0	25 % (1)	**0**
Epistaxis (16)	6.25 % (1)	0	0	**6.25 % (1)**
Eye perforation (16)	6.25 % (1)	0	0	**6.25 % (1)**

supine photon workflows. These values are comparable to those published for other upright or hexapod-based systems. Continued monitoring will determine whether the observed improvement persists as the program expands to include more patients and tumor sites.

The dosimetric findings from our analysis align with and extend previous work highlighting the advantages of proton therapy in re-irradiation settings [2,7,21]. Based on the results of the entire cohort, the median maximum doses to the brainstem and spinal cord decreased to 2.8 Gy(RBE) and 13.8 Gy(RBE), respectively. This is compared to the photon IMRT levels of 19.8 Gy and 17.8 Gy ($p < 0.001$ and $p < 0.02$), highlighting the ability of this modality to minimize exposure to previously irradiated normal tissues while delivering therapeutic doses to the target.

A four-modality substudy directly compared upright protons with supine protons delivered on a rotating gantry, as well as with photon IMRT in both postures. Upright protons provided non-inferior—and, in select cases, superior—OAR sparing without loss of target-volume coverage when the anatomy was favorable. In Patient C, the mean doses to the mandible and oral cavity fell by 23 % and 18 %, respectively. This supports the anatomical hypothesis that vertical posture retracts the tongue base and anteriorly displaces the mandible. This shortens the proton range to posterior pharyngeal structures. However, Patient D experienced an increase in laryngeal dose despite improved spinal cord sparing. This indicates that patient-specific anatomical shifts, rather than intrinsic beam quality, determine the net benefit of the upright approach. The roughly eight percent absolute conformity penalty observed in two cases suggests that beam-angle limitations and posture-induced organ motion must be compensated for through robust optimization, adaptive planning, and refined immobilization.

Early clinical results are equally encouraging. At three months, 64.3 % of evaluable patients achieved a complete response, and 21.4 % achieved a partial response. These finding are comparable to or exceed those reported in gantry-based proton re-irradiation series series [6,7,21,22]. McDonald et al. [21] reported similar response rates in patients with recurrent HN cancers treated with conventional PT systems and a study by Phan et al [22] highlighted the importance of patient selection and risk assessment, as balancing local control with minimizing toxicity is a challenge in re-irradiation settings. Consistent with Romesser et al. [2], acute grade ≥ 3 toxicity rates were lower than typical for photon re-irradiation, suggesting that advanced proton techniques can enhance disease control and safety. However, several deaths occurred, likely reflecting the patients' overall disease burden and treatment.Although none were definitively attributed to the proton system or upright positioning, these events highlight the complexity of treating heavily pretreated patients. A large cohort study by Lee et al. [23] found that while PT-ReRT offers longer survival compared to photon-based re-irradiation in aggressive cases, surviving patients remain at risk for early and late complications. This highlights the need for continued refinement of patient selection and monitoring protocols.

Implementing the upright workflow required adapting contouring protocols, developing dedicated immobilization devices, and thoroughly validating the robotic chair's accuracy, as recently reported by Feldman et al. [13] and continued in this study. These practical considerations are pivotal for centers contemplating the adoption of comparable technology.

However, the interim nature of the analysis, modest sample size, and limited follow-up restrict firm conclusions about long-term outcomes. The patient cohort is heterogeneous, encompassing various tumor sites, histologies, and prior treatment histories, which may confound interpretation. Ongoing accrual will allow for multivariate modeling to identify geometric predictors of an upright advantage. Extended follow-up and functional imaging in both postures will clarify intrafraction stability and late toxicity. Nevertheless, the consistent dosimetric advantages and the early promising clinical outcomes provide a strong rationale for further investigating this approach.

Conclusion

This interim analysis shows that chair-based, upright, image-guided, adaptive proton therapy is a feasible, safe, and dosimetrically advantageous option for the re-irradiation of head-and-neck and brain tumors. Early outcomes—including a complete (64.3 %) or partial (21.4 %) response and a low incidence of high-grade acute toxicity—are comparable to those of published series using gantry-based proton therapy. The four-way planning substudy confirms that, in most geometries, upright delivery can match or exceed gantry-based supine protons in sparing critical neural and swallowing structures without compromising target-volume coverage. By eliminating the rotating gantry, the platform reduces capital costs and facility footprint, which could improve the cost-effectiveness of proton re-irradiation.

Integrating vertical CT imaging with a robotic six-degree-of-freedom chair advances upright workflow significantly, but introduces new requirements for immobilization and quality assurance that warrant ongoing optimization. As accrual continues for the planned 50-patient cohort, extended follow-up will clarify durable tumor control, late toxicity, and quality-of-life benefits. Future work should refine anatomical selection criteria, quantify robustness margins unique to the upright posture, and establish consensus quality assurance standards so that this emerging paradigm can be safely adopted across multiple centers.

Funding Statement
P-Cure Ltd./Inc. provided financial support for this study.

CRediT authorship contribution statement

Philip Blumenfeld: Writing – review & editing, Writing – original draft, Methodology, Investigation, Formal analysis, Data curation, Conceptualization, Validation. **Alexander Pryanichnikov:** Writing – review & editing, Writing – original draft, Visualization, Validation, Methodology, Formal analysis, Conceptualization, Investigation. **Yair Hillman:** Writing – review & editing, Writing – original draft, Methodology, Investigation, Formal analysis, Data curation. **Ella Wajnryt:** Writing – review & editing, Writing – original draft, Methodology, Investigation, Formal analysis, Data curation. **Aviad Berger:** Writing – review & editing, Writing – original draft, Investigation, Formal analysis, Data curation. **Shimshon Winograd:** Data curation, Formal analysis, Software, Visualization, Writing – review & editing, Methodology. **Marc Wygoda:** Writing – review & editing, Writing – original draft, Supervision, Investigation, Conceptualization. **Ayman Salhab:** Writing – review & editing, Writing – original draft, Investigation, Conceptualization, Data curation. **Marcel Fang:** Writing – review & editing, Writing – original draft, Validation, Investigation, Data curation. **Jon Feldman:** Writing – review & editing, Writing – original draft, Validation, Project administration, Methodology, Formal analysis, Data curation. **Aron Popovtzer:** Writing – review & editing, Writing – original draft, Validation, Supervision, Project administration, Conceptualization, Methodology.

Declaration of competing interest

The authors declare that they have no known competing financial interests or personal relationships that could have appeared to influence the work reported in this paper.

Appendix A. Supplementary data

Supplementary data to this article can be found online at https://doi.org/10.1016/j.radonc.2025.111097.

References

[1] Chen AM, Harris JP, Nabar R, Tjoa T, Haidar Y, Armstrong WB. Re-irradiation versus systemic therapy for the management of local-regionally recurrent head and neck cancer. Radiother Oncol 2024;196:110278. https://doi.org/10.1016/j.radonc.2024.110278.

[2] Romesser PB, Cahlon O, Scher ED, Hug EB, Sine K, DeSelm C, et al. Proton Beam Reirradiation for Recurrent Head and Neck Cancer: Multi-institutional Report on Feasibility and Early Outcomes. Int J Radiat Oncol Biol Phys 2016;95:386–95. https://doi.org/10.1016/j.ijrobp.2016.02.036.

[3] Willmann J, Andratschke N, Klußmann JP, Gschwend JE, Tabatabai G, Niyazi M. Criteria for Re-Irradiation. Dtsch Arztebl Int 2024;121:725–32. https://doi.org/10.3238/arztebl.m2024.0156.

[4] Beddok A, Vela A, Calugaru V, Tessonnier T, Kubes J, Dutheil P, et al. Proton therapy for head and neck squamous cell carcinomas: a review of the physical and clinical challenges. Radiother Oncol 2020;147:30–9. https://doi.org/10.1016/j.radonc.2020.03.006.

[5] Paganetti H. Range uncertainties in proton therapy and the role of Monte Carlo simulations. Phys Med Biol 2012;57:R99–117. https://doi.org/10.1088/0031-9155/57/11/R99.

[6] Lemaeva A, Gulidov I, Smyk D, et al. A single-center experience of the upright proton therapy for skull-base chordomas and chondrosarcomas: Updated results. Clin Transl Radiat Oncol 2024;48:100814. https://doi.org/10.1016/j.ctro.2024.100814.

[7] Deek MP, et al. Proton therapy re-irradiation for head and neck cancers: Outcomes and prognostic factors. Cancer 2021;127:213–24. https://doi.org/10.1002/cncr.33250.

[8] Mohan R. A review of proton therapy - current status and future directions. Precis Radiat Oncol 2022;6:164–76. https://doi.org/10.1002/pro6.1149.

[9] Devicienti S, Strigari L, D'Andrea M, Benassi M, Dimiccoli V, Portaluri M. Patient positioning in the proton radiotherapy era. J Exp Clin Cancer Res 2010;29:47. https://doi.org/10.1186/1756-9966-29-47.

[10] Volz L, Sheng Y, Durante M, Graeff C. Considerations for upright particle therapy patient positioning and associated image guidance. Front Oncol 2022;12:930850. https://doi.org/10.3389/fonc.2022.930850.

[11] Yan S, Lu HM, Flanz J, Adams J, Trofimov A, Bortfeld T. Reassessment of the necessity of the proton gantry: Analysis of beam orientations from 4332 treatments at the Massachusetts General Hospital proton center over the past 10 years. Int J Radiat Oncol Biol Phys 2016;95:224–33. https://doi.org/10.1016/j.ijrobp.2015.09.033.

[12] Feldman J, Pryanichnikov A, Achkienasi A, et al. Commissioning of a novel gantryless proton therapy system. Front Oncol 2024;14:1417393. https://doi.org/10.3389/fonc.2024.1417393.

[13] Feldman J, Pryanichnikov A, Shwartz D, et al. Study of upright patient positioning reproducibility in image-guided proton therapy for head and neck cancers. Radiother Oncol 2024;201:110572. https://doi.org/10.1016/j.radonc.2024.110572.

[14] Lane SA, Slater JM, Yang GY. Image-Guided Proton Therapy: a Comprehensive Review. Cancers (Basel) 2023;15:2555. https://doi.org/10.3390/cancers15092555.

[15] van Herk M. Errors and margins in radiotherapy. Semin Radiat Oncol 2004;14:52–64. https://doi.org/10.1053/j.semradonc.2003.10.003.

[16] Palm RF, Oliver DE, Yang GQ, et al. Impact of type of treatment center and access to care on mortality and survival for skull base chordoma and chondrosarcoma. J Radiat Oncol 2020;15:30–9. https://doi.org/10.1016/j.radonc.2020.03.006.

[17] Marano J, Kissick MW, Underwood TSA, Laub SJ, Lis M, Schreuder AN, et al. Relative thoracic changes from supine to upright patient position: a proton collaborative group study. J Appl Clin Med Phys 2023;24:e14129. https://doi.org/10.1002/acm2.14129.

[18] Boisbouvier S, Boucaud A, Tanguy R, Grégoire V. Upright patient positioning for pelvic radiotherapy treatments. Tech Innov Patient Support Radiat Oncol 2022;24:124–30. https://doi.org/10.1016/j.tipsro.2022.11.003.

[19] Pryanichnikov AA, Sokunov VV, Shemyakov AE. Some results of the Clinical use of the Proton Therapy complex "Prometheus". Phys Part Nuclei Lett 2018;15:981–5. https://doi.org/10.1134/S1547477118070592.

[20] Gordon K, Gulidov I, Smyk D, Semenov A, Golubev K, Lemaeva A, et al. Upright proton therapy for esthesioneuroblastoma: a single-institution experience. Front Oncol 2024;14:1348291. https://doi.org/10.3389/fonc.2024.1348291.

[21] McDonald MW, Zolali-Meybodi O, Lehnert SJ, Estabrook NC, Liu Y, Cohen-Gadol AA, et al. Int J Radiat Oncol Biol Phys 2016;96:808–19. https://doi.org/10.1016/j.ijrobp.2016.07.037.

[22] Phan J, Sio TT, Nguyen TP, Takiar V, Gunn GB, Garden AS, et al. Reirradiation of Head and Neck Cancers with Proton Therapy: Outcomes and analyses. Int J Radiat Oncol Biol Phys 2016;96:30–41. https://doi.org/10.1016/j.ijrobp.2016.03.053.

[23] Lee A, Woods R, Mahfouz A, Kitpanit S, Cartano O, Mohamed N, et al. Evaluation of Proton Therapy Reirradiation for patients with Recurrent Head and Neck Squamous Cell Carcinoma. JAMA Netw Open 2023;6:e2250607. https://doi.org/10.1001/jamanetworkopen.2022.50607.